Microstructural and rheological investigation of upcycled metal-organic frameworks stabilized Pickering emulsions

Fabrice Lorignon, Alban Gossard, Michaël Carboni, Daniel Meyer

Microstructural and rheological investigation of upcycled metal-organic frameworks stabilized Pickering emulsions

Fabrice Lorignon[a,b], Alban Gossard[b]*, Michaël Carboni[a], Daniel Meyer[a]

[a]ICSM, CEA, Univ Montpellier, CNRS, ENSCM, BP 17171, 30207 Bagnols-sur-Cèze Cedex, France

[b]CEA, DES, ISEC, DMRC, Univ Montpellier, Marcoule, France

* Corresponding author: A. Gossard

Postal address:

Laboratoire des Procédés Supercritiques et de Décontamination

CEA Marcoule

ISEC/DMRC/STDC/LPSD Bât51

30207 Bagnols-sur-Cèze Cedex

Phone: +334 66 33 91 34

E-mail address: alban.gossard@cea.fr

Abstract

Hypothesis

Stabilizing Pickering emulsions with metal-organic frameworks (MOFs) is a known way to incorporate them into hierarchically porous materials. Studies generally focus on their final properties and emulsion microstructures are rarely precisely described. Our hypothesis was that characterizing the microstructural and rheological properties of Pickering emulsions stabilized solely by Al-based MOFs (MIL-96) particles would provide insights into how to control their stability and workability for potential industrial applications.

Experiments

MIL-96(Al) particles, obtained from Li-ion battery waste were used to stabilize paraffin-in-water Pickering emulsions. The influence of the formulation parameters (paraffin/water volume ratio and MIL-96(Al) content) were investigated and the emulsions were analysed using optical microscopy, cryo-scanning electron microscopy and rheological measurements.

Findings

MIL-96(Al) efficiently stabilized paraffin-in-water emulsions with up to 80% of internal phase. The emulsions with a low paraffin volume fraction had large droplets and a fluid gel-like texture. The emulsions with higher paraffin volume fractions were more compact and had two-step flow curves. In this system, excess MIL-96(Al) particles aggregated in the continuous phase as flocs interact with particles adsorbed at the paraffin-water interface, creating a secondary network that has to be broken for flow to resume. This behaviour may be interesting to investigate in other MOF-stabilized emulsions.

Keywords

Metal-organic frameworks; Shaping; Pickering emulsion; Rheology; Upcycling strategy

1. Introduction

Metal-organic frameworks (MOFs) are a class of hybrid organic-inorganic materials with high crystallinity, large surface areas, excellent chemical and thermal stability and a well-defined porosity [1,2]. Outstanding functionalities can be achieved by appropriately tailoring the nature of the organic linker and of the metal nodes [3]. These materials have thus found a wide range of applications, such as in catalysis [4,5], gas separation or storage [6,7], and drug delivery [8,9]. However, the fact that MOFs are typically produced as crystalline powders makes them unsuitable for a large utilisation outside the lab. To overcome this limitation, recent studies have focused on shaping MOFs as monoliths [10,11], ideally with a hierarchically porous structure [12]. Different routes have been proposed to shape MOFs in this way, namely various mechanical processes (granulation, pressing, extrusion or spray drying), finely controlled metal-organic gel formation, thin film deposition, and sacrificial templating.

Emulsions are a type of sacrificial template that could be used to produce monolithic materials with hierarchical porosity [13–18]. In these syntheses, MOFs are first mixed into an emulsion containing precursors of a structural material (generally polymeric) in the continuous phase. A macroporous monolithic material can then be obtained by growing a solid skeleton in the continuous phase (by polymerization) and eliminating the internal phase. The solidified continuous phase provides the overall structure of the material and the diameters of the macropores depend on the size of the droplets in the initial emulsion. The MOFs are thereby embedded in the solid structure, yielding a hybrid and hierarchically porous materials. Stabilizing the emulsion is a key step of the synthesis. MOFs are either dispersed in the continuous phase of a surfactant-stabilized emulsion or directly use as emulsifier without a surfactant. This is possible because MOFs amphiphilic properties mean that they can adsorb to oil-water interfaces and thus stabilize Pickering emulsions [19–22]. Depending on their wettability indeed, solid particles can adsorb to the interface of two immiscible fluids, reducing the interfacial tension and stabilizing droplets. There is a real interest in using MOFs to stabilize the precursor of the final material (the Pickering emulsion) because this ensures the MOF particles are positioned on the surfaces of the resulting macroporous network [15,16]. On the contrary, when MOFs

particles are dispersed in a surfactant-stabilized emulsion, the MOFs become embedded in the walls of the material, limiting their accessibility [13,14,23].

To the best of our knowledge, the stabilisation of both oil-in-water (O/W) and water-in-oil (W/O) Pickering emulsions by MOFs was demonstrated for the first time by Xiao et al. [24]. MOF-stabilized emulsions have since been investigated for the synthesis of hybrid materials designed for microencapsulation [23,25,26] and wastewater treatment [17,18]. Different MOFs (UiO-66, HKUST-1 or ZIF-8) have been shown to have exceptional stabilization properties in O/W and W/O emulsions [24,26,27], CO_2-in-water emulsions [28,29] and even ionic liquid-in-water emulsions [30]. The majority of articles on MOF-stabilized emulsions focus on the properties and applications of the final material and there have only been a few studies [27,30] devoted to the microstructural characteristics of the MOF-stabilized Pickering emulsions themselves. This is surprising because controlling the properties of the emulsion is crucial both to optimizing the microstructural design of the MOF-functionalized materials and to ensuring that the fluid is workable into an appropriate structure (e.g. by extrusion or additive manufacturing) [31,32] without any degradation of the internal microstructure.

In this context, the objective of the present study was to observe and characterize for the first time the microstructure of O/W emulsions exclusively stabilized by MIL-96(Al) MOF particles obtained by an upcycle approach as recently demonstrated by Cognet et al. [33], and were used here as model MOFs to stabilize paraffin-in-water emulsions. The microstructure of the emulsions was investigated at different MOF concentrations and paraffin/water volume ratios by using optical microscopy, rheological measurements and cryo-scanning electron microscopy (cryo-SEM) observations.

2. Materials and methods

The large scale synthesis of MIL-96(Al) particles was performed as described in the literature [33]. Protocols and characterizations are provided in Supporting Material.

.

2.1. Formulation of Pickering emulsions stabilized by MIL-96(Al)

All the steps in this procedure were performed at room temperature. The MOF particles were first dispersed in ultrapure water for 30 min in an ultrasonic bath. The MOF concentration (w_{MOF}) was defined by weight (wt.%), namely the mass of MOFs (m_{MOFs}) divided by the total mass of oil and water:

$$w_{\mathrm{MOF}} = \frac{\mathrm{m_{MOF}}}{\mathrm{V_{oil}} \cdot \rho_{\mathrm{oil}} + \mathrm{V_{water}} \cdot \rho_{\mathrm{water}}} \cdot 100 \quad (1)$$

with V_{oil} and V_{water} the volume of the oil and water phase and ρ_{oil} and ρ_{water} the density of the oil and water phase respectively.

The MOF concentration was varied from 1 to 5 wt.%. A volume of paraffin (a mineral oil) was then added before shearing the mixture using an IKA Ultra Turrax T25 homogenizer with a single rotor (S25N-10 G) at 15000 revolutions per minute for 3 min. Different emulsions were produced by modifying the paraffin volume fraction ϕ_v from 0.5 to 0.8 v/v.

2.2. Characterisations of the Pickering emulsions stabilized by MIL-96(Al) particles

Droplet sizes in the emulsions were measured by optical microscopy (Nikon Eclipse LV 100) at 5× and 10× magnification. The emulsion droplets were placed between two glass lamellas sufficiently spaced to avoid crushing them. The distribution of droplet sizes was obtained using image analysis software (NIS Elements D). The internal structure of the emulsions was analyzed by cryo-SEM 250 FEG microscope. One drop of the emulsion was frozen in nitrogen slush at -220°C. The frozen drop was transferred under vacuum to the cryo-fracture apparatus (Quorum PP3000T Cryo Transfer System) chamber where it was fractured at -145°C. The temperature was then increased to -95°C and maintained at this temperature during 20 min for sublimation. It was then metalized with Pd for 60 s and introduced into the cryo-SEM Quanta 250 FEG microscope chamber where it was maintained at -145°C during the observation, operating at 5 kV accelerating voltage as described by Payre et al [34].

The rheological properties of the emulsions were investigated using a TA instruments Discovery Hybrid Rheometer (DHR 1). The viscoelastic moduli (G' and G'') of the emulsions were determined in oscillation-amplitude mode, at a frequency of 1 Hz and with a strain varying from 0.005 to 100 %. This frequency was specifically chosen to ensure a plateau was observed in the linear viscoelastic domain at which the storage modulus (G'_0) was measured. The instrument was set up with two rough parallel plates 40 mm in diameter and 1000 µm apart. The flow curves of the emulsions (viscosity or shear stress as a function of the shear rate) were measured in flow-ramp mode by increasing the shear rate by 0.01 to 1000 s^{-1} over 120 s. The measurement periods were preceded by 30 s at 0.01 s^{-1} to initiate the flow.

3. Results and discussion

The MIL-96(Al) powder consisted of particles 300 to 450 nm in diameter (Fig. SI 1.a) with good crystallinity (Fig. SI 1.b) matching to the as synthesize MIL-96(Al) [35] with high porosity of 650 $m^2 \cdot g^{-1}$ (Fig. SI 1.c). Fig. SI 2 shows the time evolution of the interfacial tension between paraffin and a suspension of 125 $mg \cdot L^{-1}$ MIL-96(Al) in water. The decrease in the interfacial tension demonstrated the adsorption of MIL-96(Al) particles at the paraffin–water interface. Indeed, due to their amphiphilic properties, MIL-96 (Al) particles present a partial wetting of both water and paraffin and are thus theoretically able to stabilize Pickering emulsions between these liquids [22,24,36].

3.1. O/W emulsions stabilised by MIL-96(Al) particles: general observations

Fig. 1.a and 1.b show the paraffin–water emulsions obtained with different paraffin volume fractions and different MIL-96(Al) concentrations. The particles are adsorbed at the interface, reducing the interfacial tension and the resulting emulsions are highly stable (several months). These results suggest that paraffin-in-water emulsions can be stabilized with as little as 1 wt.% MIL-96(Al) and until high volume fractions of paraffin, highlighting the remarkable emulsifying properties of the MIL-96(Al) particles. Note here that increasing the paraffin volume fraction over than 0.85 leads to a demulsification of the studied system regardless of the MIL-96(Al) weight percentage (Fig. SI 3.a).

Comparing the emulsions with different oil volume fractions, those with a ϕ_v < 0.7 were macroscopically more fluid and flow readily (Fig. 1.a). Note that adding more than 8 wt.% MIL-96(Al) led to sedimentation of the materials in the emulsion. The high internal phase emulsions (HIPEs), those with ϕ_v > 0.7 (Fig. 1.b), were much more viscous and behave more like gels, making it possible to increase the MIL-96(Al) concentration without sedimentation.

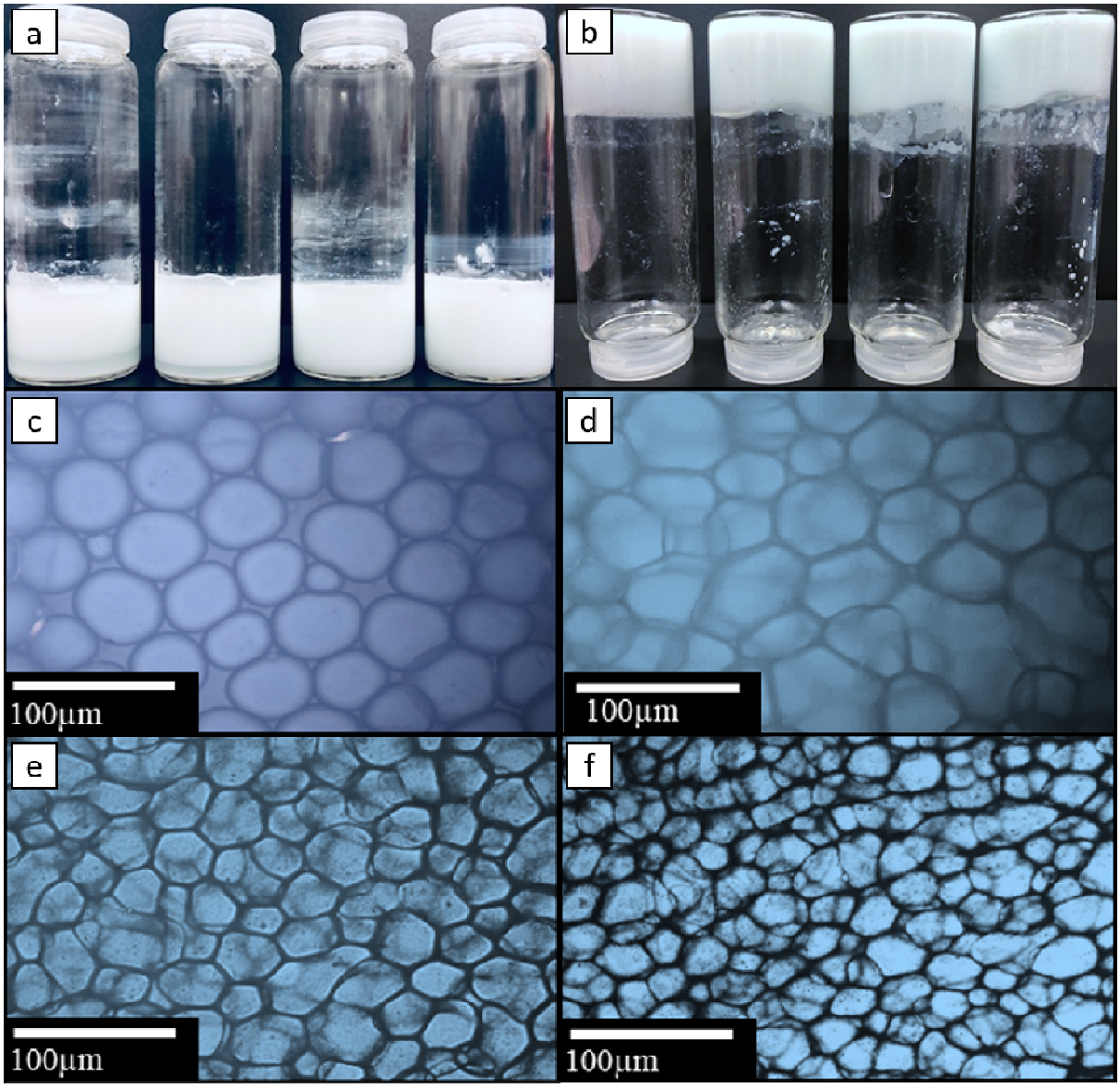

Fig.1. (a) Pickering emulsions with 2.5 wt.% MIL-96(Al) and different paraffin volume ratios: from left to right, ϕ_v = 0.5, 0.6, 0.7 and 0.8. (b) Pickering emulsions with ϕ_v = 0.8 and different concentrations of MIL-96(Al): from left to right, $w_{\mathrm{MOF}} = 1$, 2, 3.5 and 5 wt.%. Optical micrographs of emulsions with 5 wt.% MIL-96(Al) and paraffin volume ratios of (c) 0.5, (d) 0.6, (e) 0.7, and (f) 0.8.

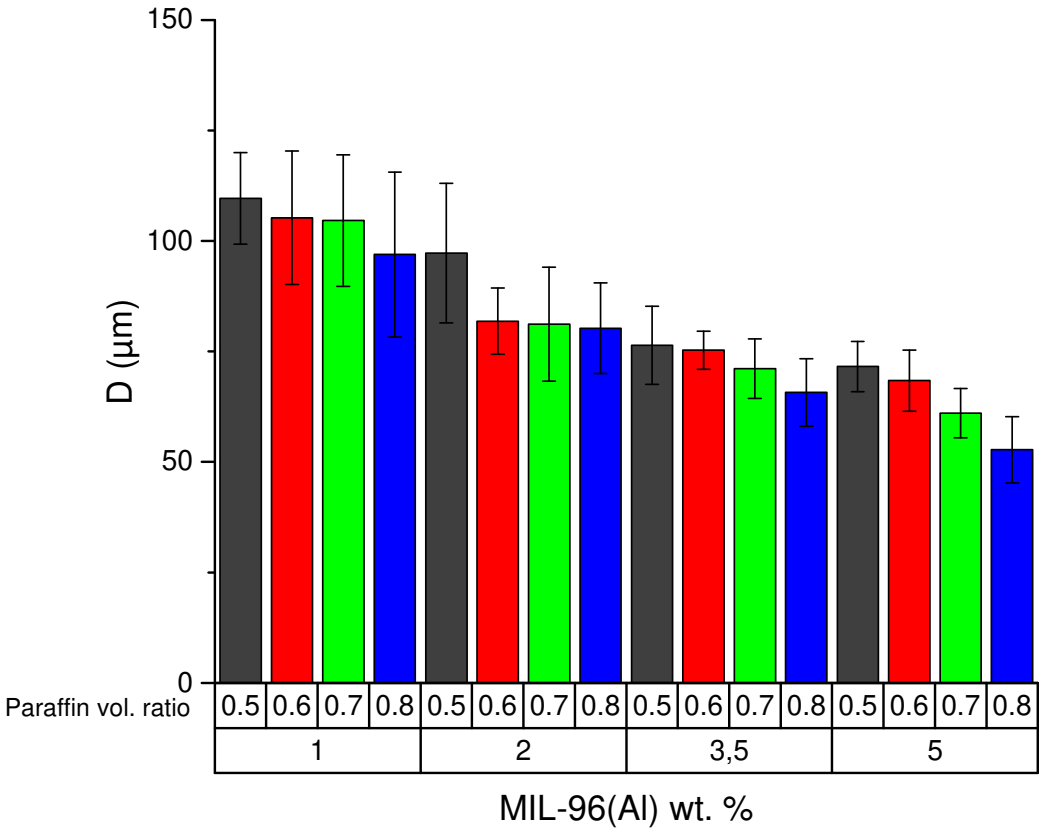

Fig. 2. Mean droplet sizes (D) in paraffin-in-water emulsions stabilized by MIL-96(Al) as a function of the paraffin volume ratio and the MIL-96(Al) concentration. The error bars represent standard deviations.

3.2. Characterization of the droplet network

Fig. 1.c-f show optical micrographs of emulsions with 5 wt.% MIL-96(Al) and different paraffin volume ratios, while Fig. 2 shows how the mean droplet size varies as a function of the paraffin volume ratio and the MIL-96(Al) concentration. The average diameter of the droplets decreases as the MOF concentration increases for all emulsions, regardless of the paraffin volume fraction. For the emulsions with $\phi_v = 0.5$, the average droplet size was 109 µm at 1 wt.% MIL-96(Al), compared with 71 µm at 5 wt.% MIL-96(Al). At lower MOF concentrations (below 0.5 wt.%), it is observed that emulsions are no more stable (Fig. SI 3.b). At $\phi_v = 0.8$, the corresponding average droplet sizes were 96 and 52 µm respectively, indicating that the droplets become slightly smaller at higher volume fractions.

Comparing the images in Fig. 1.c-f shows that in the emulsions with 5 wt.% MIL-96(Al), the droplets are more tightly packed at higher paraffin volume ratios. This is consistent with the gel-like behaviour of the HIPEs, the high paraffin volume ratio leading to a close-packed system with reduced droplet mobility in the continuous phase. Fig. 1.c-f also show that the droplets become increasingly deformed under the effect of their neighbours at higher paraffin volume ratios, creating a constrained network of hexagonal-shaped droplets.

3.3. Limited coalescence

The fact that these emulsions have narrow particle size distributions – standard deviations of 10–15µm at 5 wt. % MIL-96(Al) and a minimum droplet size of around 50 µm (Fig. 2) – is suggestive of a limited coalescence process. According to Whitesides and Ross [37] indeed, coalescence ceases in such systems when the surfaces of the droplets become fully covered by particles. In limited coalescence emulsions, it has been demonstrated that the inverse mean diameter (D) of the droplets increases linearly with the particle-to-oil weight ratio [38,39]:

$$\frac{1}{D} = \frac{a_p}{6 \cdot \rho_p \cdot v_p \cdot \tau} \cdot \frac{m_p}{V_{oil}} \quad (2)$$

In this equation, m_p is the mass of the particles, V_{oil} the volume of oil, τ is the proportion of the surface of the droplets covered by particles (coalescence stops when τ nears 1) and a_p, v_p and ρ_p are respectively the surface area, volume and density of the particles. Fig. 3 shows that the inverse mean droplet diameter increases linearly with the ratio of the mass of the particles and the volume of paraffin in the emulsion, confirming that the emulsions equilibrate by limited coalescence. The slopes and intercepts of the straight lines fitted to the data (Fig. SI 4) are listed in Table SI 1 and can be used to determine the coverage rate at a given MIL-96(AL)/paraffin ratio, assuming that the particles are irreversibly adsorbed at the interface and that coalescence does indeed stop when the surface of the droplets is completely covered [39,40].

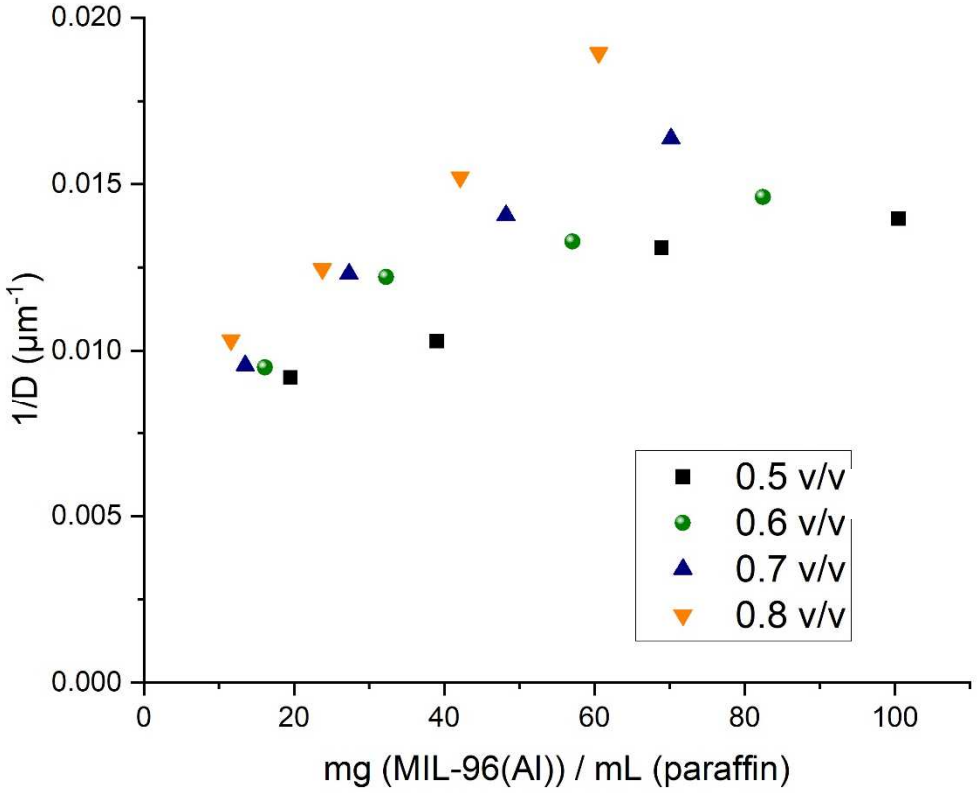

Fig.3. Inverse mean droplet diameter (1/D) as a function of mass-to-volume ratio of MIL-96(Al) particles and paraffin in emulsions with paraffin volume ratios of 0.5–0.8 v/v.

Whitesides and Ross describe limited coalescence as a sufficiently robust process that does not depend on the initial agitation state or solid mass content of the material [37]. Although according to Eq. (2), the lines fitted through the data in Fig. SI 4 should pass through the origin, the intercept in each case is ~0.009 μm^{-1} (Table SI 1). This is probably because the system is not ideal, the MIL-96(Al) particles being of different sizes (300 to 450 nm), because they were prepared from recycled material, and ellipsoidal in shape rather than perfectly spherical (Fig. SI 1a)

While the relationship is close to perfectly linear for the emulsion with ϕ_v = 0.8, the slope becomes progressively shallower at higher MIL-96(Al) contents for the emulsions with ϕ_v = 0.5, 0.6 and 0.7 (Fig. 3). Since the parameters a_p, v_p and ρ_p are constants, this slight decrease suggests that the coverage rate increases when the MIL-96(Al) concentration is increased. The slopes of the lines also increase overall with the paraffin volume ratio (Fig. 3 and Table SI 1), meaning that the coverage rate at a given MIL-96(Al) content is lower in the emulsions with higher paraffin contents. This may

be because the droplets in these emulsions are only separated by a thin layer of continuous phase (Fig. 1.c-f), which is more susceptible to jamming by MIL-96(Al) particle aggregates, inducing a decrease in the coverage rate of the paraffin–water interface.

3.4. Rheological properties of the MIL-96(Al) stabilized emulsions

3.4.1. Behaviour of the emulsions in the linear viscoelastic regime from oscillatory measurements

Oscillatory rheological measurements on the emulsions confirmed their gel-like properties shown in Fig. 1.a-b. The storage modulus of these emulsions is plotted in Fig. 4 as a function of their MIL-96(Al) weight percentage.

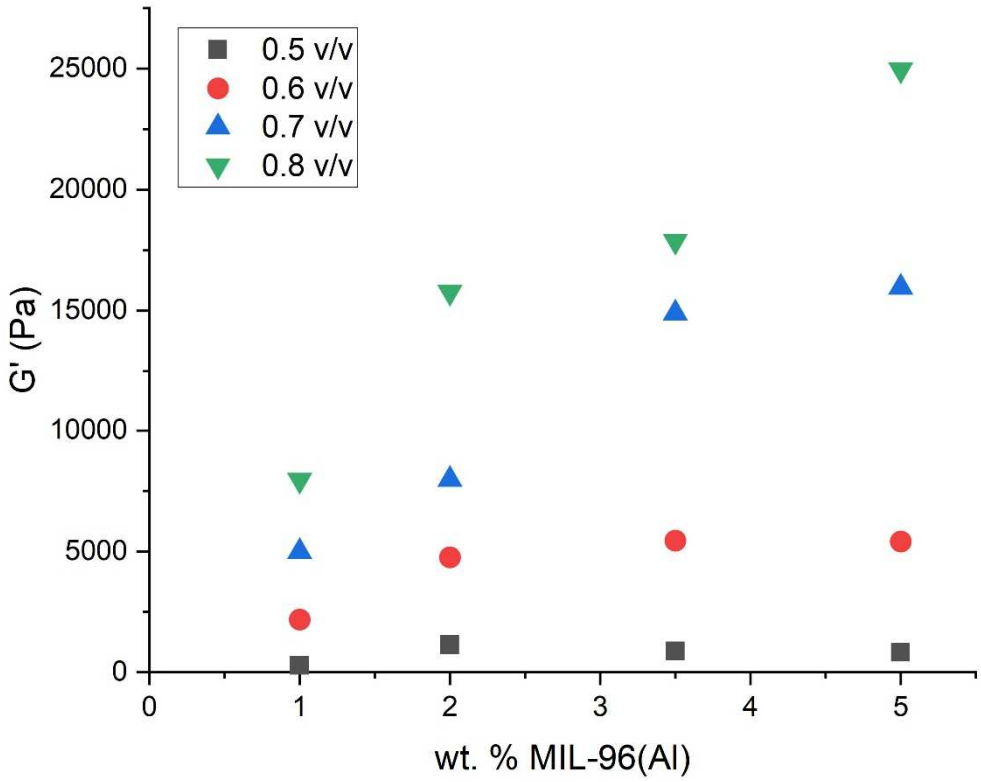

Fig. 4. Storage modulus (G'_0) as a function of MIL-96 concentration (wt.%) for emulsions with different paraffin volume ratios.

In the linear viscoelastic regime, the storage modulus is much higher than the loss modulus for all emulsions (Fig. SI 5), reflecting their high elasticity and physical stability (over a year). The storage moduli of Pickering emulsion are typically much higher than those of emulsions stabilized by organic surfactants, which tend to be more creamy and viscous [41]. Indeed, the particles adsorbed at the oil/water interface and dispersed in the aqueous phase create a viscoelastic film that forms a physical barrier, which hinders coalescence and prevents droplet migration and sedimentation [42–46]. The greater elasticity (higher G'_0) at a given MIL-96(Al) concentration of the emulsions with higher paraffin/water ratios (Fig. 4) indicates that increasing the paraffin content produces an emulsion with more tightly packed droplets and promotes flocculation. This more tightly packed droplet network is more resistant [42,43], and can store more energy by deformation of the droplets. Chevalier et al.'s results show that paraffin droplets in Pickering emulsions are sufficiently covered at solid particle concentrations as low as 1 wt.% [22]. In our emulsions therefore, the MIL-96(Al) particles are in excess and the behaviour and effects of these excess particles are discussed in the following sections.

At low paraffin volume fractions (ϕ_v = 0.5 and 0.6 v/v), Fig. 4 shows that increasing the MIL-96(Al) content only leads to a slight increase in the storage modulus. Although the concentration of excess MIL-96(Al) particles in the continuous phase (those that are not adsorbed at the paraffin-water interface) increases, the volume of the aqueous phase is high enough to sufficiently disperse the solid particles, even with MIL-96(Al) contents as high as 5 wt.%, such that there is no significant increase in G'_0. In the HIPEs however (ϕ_v = 0.7 and 0.8 v/v), the storage modulus increases drastically with the MIL-96(Al) loading. The emulsion network in the HIPEs is indeed strengthened through two mechanisms [47,48] [49]. First, the low continuous phase volume means that MIL-96(Al) particle aggregates can form even at low concentrations in the emulsion. Second, the high internal phase volume deforms the droplets into less spherical shapes with sharper interfaces (Fig. 1.e-f), increasing inter-droplet friction.

In summary therefore, the studied MIL-96(Al)-stabilized emulsions are networks of dispersed droplets with, depending on the formulation, more or less aggregated MOF flocs in the continuous phase. Oscillatory rheological measurements showed that G'_0 decreased markedly outside the linear

viscoelastic regime (Fig. SI 5), which is consistent with the emulsion network breaking above the critical strain threshold.

3.4.2. Flow behaviour of the MIL-96(Al)-stabilized emulsions

Fig. 5 shows how the viscosity of the emulsions varies as a function of the shear rate.

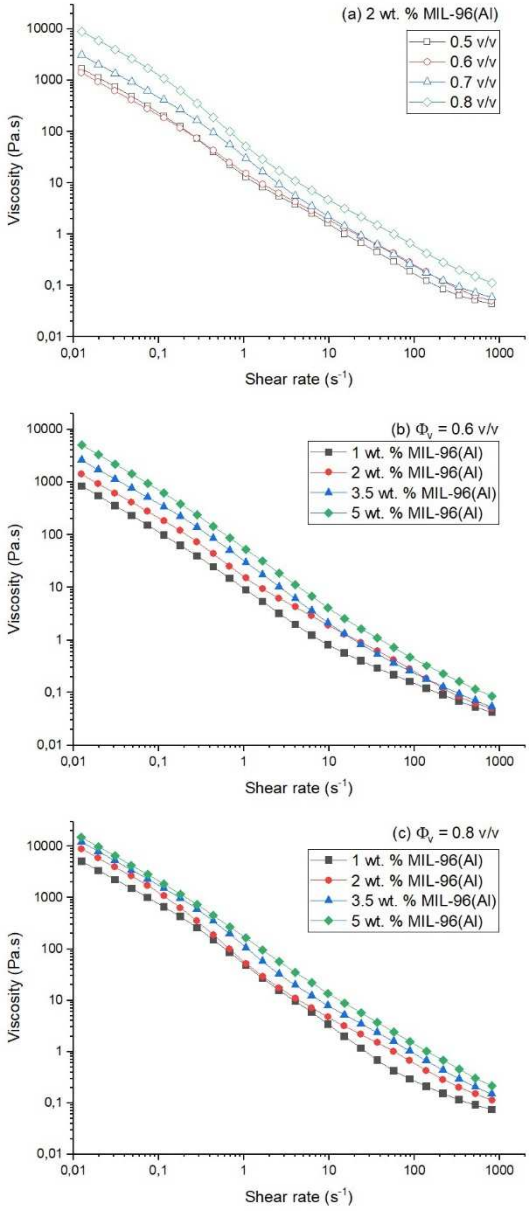

Fig. 5. Viscosity as a function of the shear rate for (a) emulsions with 2 wt.% MIL-96(Al) and different paraffin volume ratios, and (b, c) emulsions with paraffin volume ratios of 0.6 and 0.8 and different MIL-96(Al) concentrations.

As is often the case with Pickering systems [43,44,50,51], the MIL-96(Al) stabilized emulsions are pseudoplastic fluids, their apparent viscosity decreasing with increasing shear rates. Indeed, in their initial state (at rest), the droplets are randomly dispersed and compacted, making the emulsion highly viscous. As the shear rate is increased, the droplet network is deformed under hydrodynamic forces as the droplets align with the shear field and slide over each other. Furthermore, in case of particles-concentrated emulsion, the presence of free particles induces the formation of flocs in the initial emulsions. These flocs, which generally form weak aggregates by Van der Waals attraction, increase the viscosity of the emulsion but are easily broken under shear stress, which accentuates their pseudoplastic nature. This behaviour can be described by the following power law [42,43,52]:

$$\eta = K.\dot{\gamma}^{n-1} \quad (3)$$

which relates the apparent viscosity of the emulsion (η, $Pa{\cdot}s^{-1}$) to the applied shear rate ($\dot{\gamma}$, s^{-1}), via the consistency index K, a proportionality constant that depends on the structure of the gel and a power law index n directly related to the evolution of the emulsion with the shear rate.

Eq. (3) fits the flow data for all the emulsions with a high coefficient of determination ($R^2 > 0.99$; fits shown in Fig. SI 6). Table 1 lists the values of the consistency index and power law index obtained from the fits.

Table 1. Consistency index and power law index obtained by fitting the data in Fig. 5 using Eq. (3)

MIL-96(Al) concentration (wt.%)	Paraffin volume fraction (v/v)	Consistency index K	Power law index n
2	0.5	27.0	0.05
2	0.6	25.5	0.09
2	0.7	56.8	0.09
2	0.8	144.6	0.06
1	0.6	12.4	0.04
3.5	0.6	46.4	0.08
5	0.6	82.1	0.06
1	0.8	90.5	0.08

3.5	0.8	200.9	0.07
5	0.8	245.2	0.06

The low values obtained for the power law index demonstrate the high degree of shear thinning exhibited by the emulsions. The most viscous emulsions with the highest consistency indexes are those with the highest paraffin volume fractions and MIL-96(Al) concentrations. The increase in the consistency index with the paraffin volume fraction is consistent with the phenomena described above [42], namely the decrease in particle size and interparticle distance and concomitant increase in interparticle interactions, aggregation and flocculation, which all increase the viscosity and flow resistance of the emulsions.

Parts b and c of Fig. 5 show that in the emulsions with moderate ($\phi_v = 0.6$) and high ($\phi_v = 0.8$) paraffin volume fractions, the viscosity increases with the MIL-96(Al) concentration. This is because the rheological properties of these emulsions reflect not only the Pickering effect (the presence of solid particles on the surface of the drops) but also the presence of excess MOFs and MOF aggregates, which increase the viscosity of the continuous phase and thus of the emulsion as a whole [43–45]. The effect of the MIL-96(Al) concentration on the viscosity is more pronounced at the lower paraffin volume fraction: the fitted values of the consistency index increase by a factor of 6.6 between 1 and 5 wt.% with MIL-96(Al) at $\phi_v = 0.6$ but by a factor of just 2.7 at $\phi_v = 0.8$. This is because the emulsion network is already highly compact at the highest paraffin volume fraction, with the MIL-96(Al) particles tending to aggregate even at low MIL-96(Al) weight percentages. At $\phi_v = 0.6$ in contrast, the MIL-96(Al) particles transition from being well dispersed in the aqueous phase at a low weight percentage, to being highly concentrated at higher weight percentages, leading to a much sharper increase in viscosity.

Although all the relationships are well fitted overall by Eq. (3), log-log transformation of the data shows that they all deviate from the ideal behaviour at shear rates above 0.1 s^{-1} (Fig. SI 6). To investigate the microstructural origin of these deviations in more detail, the flow curves are represented in Fig. 6 as the shear stress as a function of the shear rate.

The flow curves of the MIL-96(Al) stabilized emulsions are unusual for Pickering emulsions, since the latter can typically be fitted using the Herschel-Bulkley model [43,46,48], describing the behaviour of non-Newtonian yield stress fluids. Precisions about this model are provided in the Supporting Material. Here in contrast, as the shear rate increases, the shear stress first increases, then decreases, then finally increase once more. This behaviour has been observed before in systems in which aggregates form in the continuous phase [53–56], and suggests the presence of a secondary inter-droplet network consisting of particles aggregated as flocs in the dispersed phase linked with stabilizing particles adsorbed to the oil–water interfaces. In other words, the particles that stabilize the droplets are also components of the flocs dispersed into the continuous phase. In this context, the first increase in the shear stress (at low shear rates) corresponds to the disruption of the secondary network. This floc-droplet microstructure breaks down partially above a certain stress threshold, allowing the emulsion to flow more easily under hydrodynamic forces. This maximum value can be considered a yield point that has to be overpassed for the emulsion to flow [55,56], the emulsion behaving as a solid below this value and as a liquid above it [57]. Note that this parameter is, just like the storage modulus, indicative of the physical stability of the emulsion, a sufficiently high yield stress being required to prevent any creaming under gravity [55].

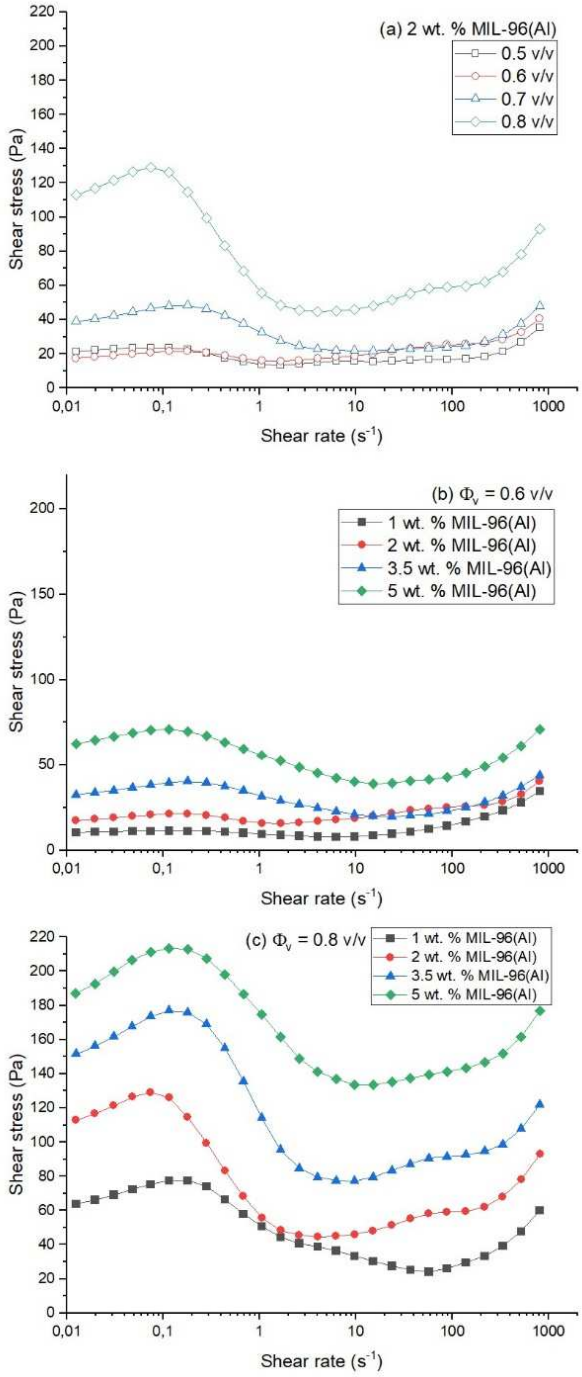

Fig.6. Shear stress as a function of the shear rate for (a) emulsions with 2 wt.% MIL-96(Al) and different paraffin volume ratios, and (b, c) emulsions with paraffin volume ratios of 0.6 and 0.8 and different MIL-96(Al) concentrations.

Fig. 6 also highlights the influence of the paraffin volume fraction and MIL-96(Al) concentration. The transition between the two regimes occurs in each case at about 0.1 s^{-1}, which is also the point at which the viscosity curves deviate from the ideal line (Fig. SI 6), but the two-step

variation is more or less pronounced depending on the paraffin volume fraction and the particle loading. At a given MIL-96(Al) concentration, the yield stress is higher and the oscillation more pronounced in the emulsions with higher paraffin volume fractions (Fig. 6a). These results can be understood in terms of the secondary floc-droplet network discussed above. When the continuous phase volume fraction is sufficiently high (ϕ_v = 0.5 and 0.6) to disperse the MIL-96(Al) particles and limit the formation of this secondary network, the flow curve resembles that of a Herschel-Bulkley fluid [43,46,48]. However, above a certain paraffin volume fraction ($\phi_v \approx 0.7$), the MIL-96(Al) particles constrained in the inter-droplet space interconnect with the droplets, and the resulting jammed network has to be disrupted before flow can begin [53,54]. The yield stress is therefore significantly higher and the subsequent rearrangement of the emulsion network once the yield stress is surpassed is also more important. This mechanism also explains why the effect of increasing the MIL-96(Al) concentration is more marked at ϕ_v = 0.8 (Fig. 6.c), than at ϕ_v = 0.6 (Fig. 6.b), the secondary network being stronger in the more constrained systems. The yield stress of the emulsion with ϕ_v = 0.8 and 1 wt.% MIL-96(Al) is thus higher that of the emulsion with ϕ_v = 0.6 and 5 wt.% MIL-96(Al).

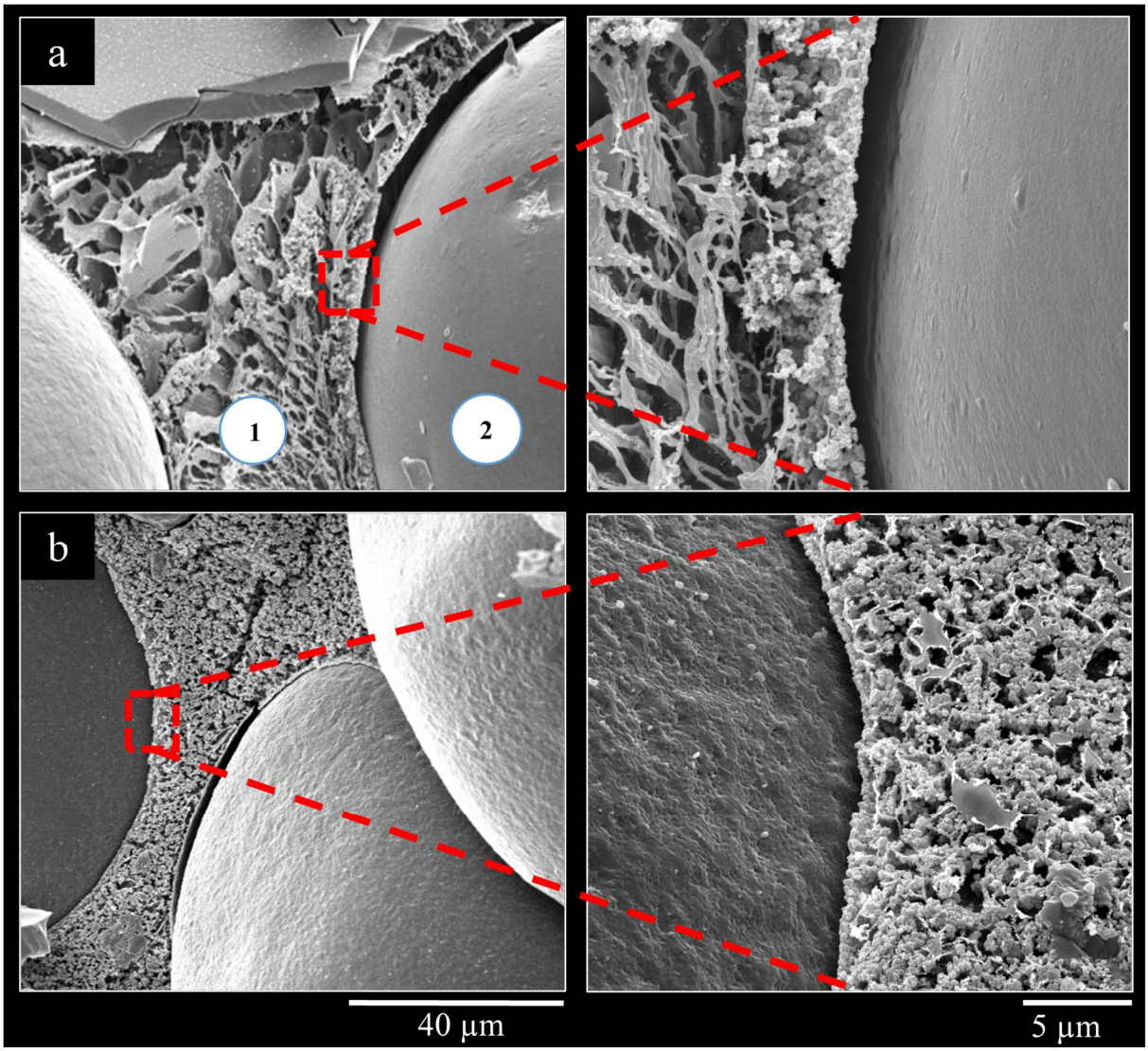

Fig. 7. Cryo scanning electron micrographs of emulsions with a paraffin volume ratio of 0.8 v/v and MIL-96(Al) concentrations of (a) 1 wt.% and (b) 3.5 wt.%. (1) Continuous aqueous phase concentrated in MIL-96(Al) and (2) oil droplet.

Fig. 7 supports this hypothesis, these are cryoSEM micrographs on which two distinct zones are highlighted, the zone (1) is the continuous phase in which the aluminium-based MOFs are organized at the interface with zone (2) which is the dispersed paraffin droplet. Note that the threadlike features are filaments of residual water from the experimental measurement procedure and, more interestingly, that the layer of MIL-96(Al) particles at the water–paraffin interface confirms that the emulsions are stabilized by a Pickering mechanism. The cryoSEM images also reveal that as the concentration of MIL-96(Al) increases, the continuous phase is more concentrated in unadsorbed

particles. The strengthening of the secondary network as the MIL-96(Al) concentration is increased as illustrated visually in Fig. 7, which shows a much denser network of MOF aggregates between the droplets in the emulsion with 3.5 wt.% MIL-96(Al) than in the one with 1 wt.% MIL-96(Al). Thus, it can be assumed that emulsions with very few and even no free particles could be formulated by perfectly controlling the ratio between the paraffin-water interface created by the shearing and the maximum surface possibly covered by the MOF particles. This could be achieved either by progressively decreasing the amount of MOF in the emulsion formulation keeping a constant shear rate or by increasing the shear rate (increase of the rotation speed of homogenizer) to create smaller droplets and thus a higher paraffin-water interface area. Such emulsions will present no secondary network and their flow behaviours should consequently be fitted using Herschel-Bulkley model. Overall, though, this investigation of the rheological properties of the emulsions demonstrates that they are more strongly affected by the paraffin volume fraction than by the concentration of solid particles.

4. Conclusions

This study brings a better understanding of the microstructure and rheological properties of emulsions with different paraffin/water volume ratios and MIL-96(Al) concentrations. The results of droplet size analyses, rheological measurements and cryoSEM observations show that when the paraffin and solid particle concentrations are low, the emulsions consist of large droplets and behave like fluid gels. Adding more particles decreases the droplet size with a slight effect on the rheological properties. However, increasing the paraffin volume fraction leads to a significant deformation of the droplets and of the emulsion network, which then becomes much more compact. The physicochemical properties of the emulsions are thus driven rather by the amount of internal phase than the solid particles concentration. Moreover, we further investigated the rheological flow of the emulsions. Compared to other Pickering emulsion systems generally described as Herschel-Bulkley fluids [43,44,48], MIL-96(Al) stabilized emulsions have an unusual two-step flow regime under increasing shear rates, with particularly pronounced variations in shear stress in the HIPEs. This behaviour is due to the excess of MOF particles that tend to aggregate, especially in the constrained continuous aqueous

phase of the HIPEs, and also to the interconnection with the particles adsorbed at the paraffin-water interface. The MOFs particles are thus considered as adsorbed as flocs at the paraffin-water interface, forming a secondary network that has to be broken for flow.

MOFs are generally good at stabilizing Pickering emulsions and readily aggregate in the continuous phase. Even if the interfacial activity of the particles can slightly differ as a function of the MOF nature, similar stabilizing mechanisms can be proposed for other Pickering emulsions stabilized with MOFs such as the "MIL" or "ZIF family" [58–61]. It is also noteworthy that the composition of the aqueous phase (presence of precursors of solid materials, pH or ionic strength) could also influence the emulsion properties by modifying inter-particles interactions. In this way, we believe that this work will be valuable for embedding MOFs in hierarchically porous materials for applications in catalysis, gas sorption or effluent decontamination using MOFs-stabilized emulsion as a precursor step. Indeed, a large majority of articles on MOF-stabilized Pickering emulsions using this strategy only focus on the properties of the final material without specific interest for the emulsification step [16,15,62]. However, the fine understanding and control of the emulsification step is crucial to design tailor-made efficient materials and to anticipate their workability for future applications. Finely controlling the droplet size should allow the formation of an interconnected macroporous network, which is a key parameter for their use in fixed processes [12,63]. Identifying the role of the MOFs amount into the stabilization mechanisms should improve their accessibility once embedded into a hierarchically porous structure and thus increase the efficiency of the material. This point is particularly an issue for the synthesis of composite including MOFs materials [13,62]. Finally, the precise information provided here on the rheological properties and the workability of the emulsions should pave the way to optimize the architectural design and shaping of MOF-containing monolithic hierarchically porous materials using extrusion or 3D printing of emulsions processes [64,65].

Acknowledgements

This work was supported by the Occitanie Region and by the CEA. The authors thank Renaud Podor for his advice and availability regarding microscopic analysis. Thanks are also directed to Naïs Mercier for the different MOFs syntheses used during this study.

References

[1] H. Furukawa, K.E. Cordova, M. O'Keeffe, O.M. Yaghi, The Chemistry and Applications of Metal-Organic Frameworks, Science. 341 (2013) 1230444–1230444. https://doi.org/10.1126/science.1230444.

[2] N. Stock, S. Biswas, Synthesis of Metal-Organic Frameworks (MOFs): Routes to Various MOF Topologies, Morphologies, and Composites, Chemical Reviews. 112 (2012) 933–969. https://doi.org/10.1021/cr200304e.

[3] Y. Cui, B. Li, H. He, W. Zhou, B. Chen, G. Qian, Metal–Organic Frameworks as Platforms for Functional Materials, Acc. Chem. Res. 49 (2016) 483–493. https://doi.org/10.1021/acs.accounts.5b00530.

[4] J. Lee, O.K. Farha, J. Roberts, K.A. Scheidt, S.T. Nguyen, J.T. Hupp, Metal–organic framework materials as catalysts, Chem. Soc. Rev. 38 (2009) 1450. https://doi.org/10.1039/b807080f.

[5] J.M. Moreno, A. Velty, U. Díaz, MOFs based on 1D structural sub-domains with Brønsted acid and redox active sites as effective bi-functional catalysts, Catal. Sci. Technol. 10 (2020) 3572–3585. https://doi.org/10.1039/D0CY00235F.

[6] H.R. Abid, G.H. Pham, H.-M. Ang, M.O. Tade, S. Wang, Adsorption of CH4 and CO2 on Zr-metal organic frameworks, Journal of Colloid and Interface Science. 366 (2012) 120–124. https://doi.org/10.1016/j.jcis.2011.09.060.

[7] J. Dhainaut, M. Bonneau, R. Ueoka, K. Kanamori, S. Furukawa, Formulation of Metal–Organic Framework Inks for the 3D Printing of Robust Microporous Solids toward High-Pressure Gas Storage and Separation, ACS Appl. Mater. Interfaces. 12 (2020) 10983–10992. https://doi.org/10.1021/acsami.9b22257.

[8] R.C. Huxford, J. Della Rocca, W. Lin, Metal–organic frameworks as potential drug carriers, Current Opinion in Chemical Biology. 14 (2010) 262–268. https://doi.org/10.1016/j.cbpa.2009.12.012.

[9] J. An, S.J. Geib, N.L. Rosi, Cation-Triggered Drug Release from a Porous Zinc−Adeninate Metal−Organic Framework, J. Am. Chem. Soc. 131 (2009) 8376–8377. https://doi.org/10.1021/ja902972w.

[10] J. Hou, A.F. Sapnik, T.D. Bennett, Metal–organic framework gels and monoliths, Chem. Sci. 11 (2020) 310–323. https://doi.org/10.1039/C9SC04961D.

[11] J. Liu, Z. Wang, R. Bi, F. Mao, K. Wang, H. Wu, X. Wang, A polythreaded Mn^{II} -MOF and its super-performances for dye adsorption and supercapacitors, Inorg. Chem. Front. 7 (2020) 718–730. https://doi.org/10.1039/C9QI01204D.

[12] F. Lorignon, A. Gossard, M. Carboni, Hierarchically porous monolithic MOFs: An ongoing challenge for industrial-scale effluent treatment, Chemical Engineering Journal. 393 (2020) 124765. https://doi.org/10.1016/j.cej.2020.124765.

[13] M. Wickenheisser, C. Janiak, Hierarchical embedding of micro-mesoporous MIL-101(Cr) in macroporous poly(2-hydroxyethyl methacrylate) high internal phase emulsions with monolithic shape for vapor adsorption applications, Microporous and Mesoporous Materials. 204 (2015) 242–250. https://doi.org/10.1016/j.micromeso.2014.11.025.

[14] M. Wickenheisser, T. Paul, C. Janiak, Prospects of monolithic MIL-MOF@poly(NIPAM)HIPE composites as water sorption materials, MICROPOROUS AND MESOPOROUS MATERIALS. 220 (2016) 258–269. https://doi.org/10.1016/j.micromeso.2015.09.008.
[15] H. Zhu, Q. Zhang, S. Zhu, Assembly of a Metal-Organic Framework into 3 D Hierarchical Porous Monoliths Using a Pickering High Internal Phase Emulsion Template, Chemistry - A European Journal. 22 (2016) 8751–8755. https://doi.org/10.1002/chem.201600313.
[16] J. Wang, H. Zhu, B.-G. Li, S. Zhu, Interconnected Porous Monolith Prepared via UiO-66 Stabilized Pickering High Internal Phase Emulsion Template, Chemistry - A European Journal. 24 (2018) 16426–16431. https://doi.org/10.1002/chem.201803628.
[17] B. Zhang, J. Zhang, C. Liu, L. Peng, X. Sang, B. Han, X. Ma, T. Luo, X. Tan, G. Yang, High-internal-phase emulsions stabilized by metal-organic frameworks and derivation of ultralight metal-organic aerogels, Scientific Reports. 6 (2016). https://doi.org/10.1038/srep21401.
[18] Y. Dong, L. Cao, J. Li, Y. Yang, J. Wang, Facile preparation of uio-66 /pam monoliths via co 2 - in-water hipes and their applications, RSC Advances. 8 (2018) 32358–32367. https://doi.org/10.1039/C8RA05809A.
[19] S.U. Pickering, CXCVI.—Emulsions, J. Chem. Soc., Trans. 91 (1907) 2001–2021. https://doi.org/10.1039/CT9079102001.
[20] Separation of solids in the surface-layers of solutions and 'suspensions' (observations on surface-membranes, bubbles, emulsions, and mechanical coagulation).—Preliminary account, Proc. R. Soc. Lond. 72 (1904) 156–164. https://doi.org/10.1098/rspl.1903.0034.
[21] R. Aveyard, B.P. Binks, J.H. Clint, Emulsions stabilised solely by colloidal particles, Advances in Colloid and Interface Science. 100–102 (2003) 503–546. https://doi.org/10.1016/S0001-8686(02)00069-6.
[22] Y. Chevalier, M.-A. Bolzinger, Emulsions stabilized with solid nanoparticles: Pickering emulsions, Colloids and Surfaces A: Physicochemical and Engineering Aspects. 439 (2013) 23–34. https://doi.org/10.1016/j.colsurfa.2013.02.054.
[23] S. Kovačič, M. Mazaj, M. Ješelnik, D. Pahovnik, E. Žagar, C. Slugovc, N.Z. Logar, Synthesis and Catalytic Performance of Hierarchically Porous MIL-100(Fe)@polyHIPE Hybrid Membranes, Macromolecular Rapid Communications. 36 (2015) 1605–1611. https://doi.org/10.1002/marc.201500241.
[24] B. Xiao, Q. Yuan, R.A. Williams, Exceptional function of nanoporous metal organic framework particles in emulsion stabilisation, CHEMICAL COMMUNICATIONS. 49 (2013) 8208–8210. https://doi.org/10.1039/c3cc43689f.
[25] J. Huo, M. Marcello, A. Garai, D. Bradshaw, MOF-Polymer Composite Microcapsules Derived from Pickering Emulsions, Adv. Mater. 25 (2013) 2717–2722. https://doi.org/10.1002/adma.201204913.
[26] P. Jin, W. Tan, J. Huo, T. Liu, Y. Liang, S. Wang, D. Bradshaw, Hierarchically porous MOF/polymer composites via interfacial nanoassembly and emulsion polymerization, Journal of Materials Chemistry A. 6 (2018) 20473–20479. https://doi.org/10.1039/C8TA06766J.
[27] P. Song, G. Natale, J. Wang, T. Bond, H. Hejazi, H. de la H. Siegler, I. Gates, Q. Lu, 2D and 3D Metal-Organic Framework at the Oil/Water Interface: A Case Study of Copper Benzenedicarboxylate, Adv. Mater. Interfaces. 6 (2019) 1801139. https://doi.org/10.1002/admi.201801139.
[28] Z. Yang, L. Cao, J. Li, J. Lin, J. Wang, Facile synthesis of Cu-BDC/Poly(N-methylol acrylamide) HIPE monoliths via CO2-in-water Emulsion stabilized by metal-organic framework, POLYMER. 153 (2018) 17–23. https://doi.org/10.1016/j.polymer.2018.07.085.
[29] C. Liu, J. Zhang, L. Zheng, J. Zhang, X. Sang, X. Kang, B. Zhang, T. Luo, X. Tan, B. Han, Metal-Organic Framework for Emulsifying Carbon Dioxide and Water, Angew. Chem. Int. Ed. 55 (2016) 11372–11376. https://doi.org/10.1002/anie.201602150.
[30] Z. Li, J. Zhang, T. Luo, X. Tan, C. Liu, X. Sang, X. Ma, B. Han, G. Yang, High internal ionic liquid phase emulsion stabilized by metal–organic frameworks, Soft Matter. 12 (2016) 8841–8846. https://doi.org/10.1039/C6SM01610C.
[31] Y. Hu, J. Wang, X. Li, X. Hu, W. Zhou, X. Dong, C. Wang, Z. Yang, B.P. Binks, Facile preparation of bioactive nanoparticle/poly(ε-caprolactone) hierarchical porous scaffolds via 3D

printing of high internal phase Pickering emulsions, Journal of Colloid and Interface Science. 545 (2019) 104–115. https://doi.org/10.1016/j.jcis.2019.03.024.
[32] X. Zhang, W. Huo, J. Liu, Y. Zhang, S. Zhang, J. Yang, 3D printing boehmite gel foams into lightweight porous ceramics with hierarchical pore structure, Journal of the European Ceramic Society. 40 (2020) 930–934. https://doi.org/10.1016/j.jeurceramsoc.2019.10.032.
[33] M. Cognet, J. Condomines, J. Cambedouzou, S. Madhavi, M. Carboni, D. Meyer, An original recycling method for Li-ion batteries through large scale production of Metal Organic Frameworks, Journal of Hazardous Materials. 385 (2020) 121603. https://doi.org/10.1016/j.jhazmat.2019.121603.
[34] B. Payre, E. Gontier, A. Jarray, Y. Martinez, J.P. Laugier, A. Delalleau, B.M. Gaillard, I. Anselme, D. Goudounèche, I. Fourquaux, M. Hemati, V. Gerbaud, M.B. Delisle, C. Guilbeau-Frugier, A new HPF specimen carrier adapter for the use of high-pressure freezing with cryoscanning electron microscope: two applications: stearic acid organization in a hydroxypropyl methylcellulose matrix and mice myocardium, Journal of Microscopy. 271 (2018) 255–265. https://doi.org/10.1111/jmi.12713.
[35] T. Loiseau, L. Lecroq, C. Volkringer, J. Marrot, G. Férey, M. Haouas, F. Taulelle, S. Bourrelly, P.L. Llewellyn, M. Latroche, MIL-96, a Porous Aluminum Trimesate 3D Structure Constructed from a Hexagonal Network of 18-Membered Rings and μ_3 -Oxo-Centered Trinuclear Units, J. Am. Chem. Soc. 128 (2006) 10223–10230. https://doi.org/10.1021/ja0621086.
[36] A. Gossard, G. Toquer, A. Grandjean, J. Causse, High-internal phase emulsions stabilized by colloidal Zr-based solid clusters, Colloids and Surfaces A: Physicochemical and Engineering Aspects. 462 (2014) 162–169. https://doi.org/10.1016/j.colsurfa.2014.09.007.
[37] T.H. Whitesides, D.S. Ross, Experimental and Theoretical Analysis of the Limited Coalescence Process: Stepwise Limited Coalescence, Journal of Colloid and Interface Science. 169 (1995) 48–59. https://doi.org/10.1006/jcis.1995.1005.
[38] V. Schmitt, M. Destribats, R. Backov, Colloidal particles as liquid dispersion stabilizer: Pickering emulsions and materials thereof, Comptes Rendus Physique. 15 (2014) 761–774. https://doi.org/10.1016/j.crhy.2014.09.010.
[39] S. Arditty, C.P. Whitby, B.P. Binks, V. Schmitt, F. Leal-Calderon, Some general features of limited coalescence in solid-stabilized emulsions, Eur. Phys. J. E. 11 (2003) 273–281. https://doi.org/10.1140/epje/i2003-10018-6.
[40] S. Arditty, V. Schmitt, J. Giermanska-Kahn, F. Leal-Calderon, Materials based on solid-stabilized emulsions, Journal of Colloid and Interface Science. 275 (2004) 659–664. https://doi.org/10.1016/j.jcis.2004.03.001.
[41] H. Tan, G. Sun, W. Lin, C. Mu, T. Ngai, Gelatin Particle-Stabilized High Internal Phase Emulsions as Nutraceutical Containers, ACS Appl. Mater. Interfaces. 6 (2014) 13977–13984. https://doi.org/10.1021/am503341j.
[42] X. Qiao, J. Zhou, B.P. Binks, X. Gong, K. Sun, Magnetorheological behavior of Pickering emulsions stabilized by surface-modified Fe3O4 nanoparticles, Colloids and Surfaces A: Physicochemical and Engineering Aspects. 412 (2012) 20–28. https://doi.org/10.1016/j.colsurfa.2012.06.026.
[43] L.G. Torres, R. Iturbe, M.J. Snowden, B.Z. Chowdhry, S.A. Leharne, Preparation of o/w emulsions stabilized by solid particles and their characterization by oscillatory rheology, Colloids and Surfaces A: Physicochemical and Engineering Aspects. 302 (2007) 439–448. https://doi.org/10.1016/j.colsurfa.2007.03.009.
[44] M.V. Tzoumaki, T. Moschakis, V. Kiosseoglou, C.G. Biliaderis, Oil-in-water emulsions stabilized by chitin nanocrystal particles, Food Hydrocolloids. 25 (2011) 1521–1529. https://doi.org/10.1016/j.foodhyd.2011.02.008.
[45] M.V. Tzoumaki, T. Moschakis, C.G. Biliaderis, Mixed aqueous chitin nanocrystal–whey protein dispersions: Microstructure and rheological behaviour, Food Hydrocolloids. 25 (2011) 935–942. https://doi.org/10.1016/j.foodhyd.2010.09.004.
[46] T. Winuprasith, M. Suphantharika, Properties and stability of oil-in-water emulsions stabilized by microfibrillated cellulose from mangosteen rind, Food Hydrocolloids. 43 (2015) 690–699. https://doi.org/10.1016/j.foodhyd.2014.07.027.

[47] Y.-T. Xu, T.-X. Liu, C.-H. Tang, Novel pickering high internal phase emulsion gels stabilized solely by soy β-conglycinin, Food Hydrocolloids. 88 (2019) 21–30. https://doi.org/10.1016/j.foodhyd.2018.09.031.
[48] F. Ye, M. Miao, S.W. Cui, B. Jiang, Z. Jin, X. Li, Characterisations of oil-in-water Pickering emulsion stabilized hydrophobic phytoglycogen nanoparticles, Food Hydrocolloids. 76 (2018) 78–87. https://doi.org/10.1016/j.foodhyd.2017.05.003.
[49] Y. Zhu, S. Huan, L. Bai, A. Ketola, X. Shi, X. Zhang, J.A. Ketoja, O.J. Rojas, High Internal Phase Oil-in-Water Pickering Emulsions Stabilized by Chitin Nanofibrils: 3D Structuring and Solid Foam, ACS Appl. Mater. Interfaces. 12 (2020) 11240–11251. https://doi.org/10.1021/acsami.9b23430.
[50] C. Qiu, J. Wang, Y. Qin, X. Xu, Z. Jin, Characterization and Mechanisms of Novel Emulsions and Nanoemulsion Gels Stabilized by Edible Cyclodextrin-Based Metal–Organic Frameworks and Glycyrrhizic Acid, Journal of Agricultural and Food Chemistry. 67 (2019) 391–398. https://doi.org/10.1021/acs.jafc.8b03065.
[51] B. Madivala, S. Vandebril, J. Fransaer, J. Vermant, Exploiting particle shape in solid stabilized emulsions, Soft Matter. 5 (2009) 1717. https://doi.org/10.1039/b816680c.
[52] Y. Liang, X. Yuan, L. Wang, X. Zhou, X. Ren, Y. Huang, M. Zhang, J. Wu, W. Wen, Highly stable and efficient electrorheological suspensions with hydrophobic interaction, Journal of Colloid and Interface Science. 564 (2020) 381–391. https://doi.org/10.1016/j.jcis.2019.12.129.
[53] B.P. Binks, J.H. Clint, C.P. Whitby, Rheological Behavior of Water-in-Oil Emulsions Stabilized by Hydrophobic Bentonite Particles, Langmuir. 21 (2005) 5307–5316. https://doi.org/10.1021/la050255w.
[54] P. Chatterjee, G.A. Sowiak, P.T. Underhill, Effect of phase change on the rheology and stability of paraffin wax-in-water Pickering emulsions, Rheol Acta. 56 (2017) 601–613. https://doi.org/10.1007/s00397-017-1021-4.
[55] J. Chen, R. Vogel, S. Werner, G. Heinrich, D. Clausse, V. Dutschk, Influence of the particle type on the rheological behavior of Pickering emulsions, Colloids and Surfaces A: Physicochemical and Engineering Aspects. 382 (2011) 238–245. https://doi.org/10.1016/j.colsurfa.2011.02.003.
[56] B.R. Midmore, Preparation of a novel silica-stabilized oil/water emulsion, Colloids and Surfaces A: Physicochemical and Engineering Aspects. 132 (1998) 257–265. https://doi.org/10.1016/S0927-7757(97)00094-0.
[57] A. Gossard, F. Frances, C. Aloin, Rheological properties of TiO2 suspensions varied by shifting the electrostatic inter-particle interactions with an organic co-solvent, Colloids and Surfaces A: Physicochemical and Engineering Aspects. 522 (2017) 425–432. https://doi.org/10.1016/j.colsurfa.2017.03.021.
[58] A. Sardari, A.A. Sabbagh Alvani, S.R. Ghaffarian, Preparation of castor oil-based fatliquoring agent via a Pickering emulsion method for use in leather coating, J Coat Technol Res. 16 (2019) 1765–1772. https://doi.org/10.1007/s11998-019-00234-1.
[59] Y. Hu, X. Song, Q. Zheng, J. Wang, J. Pei, Zeolitic imidazolate framework-67 for shape stabilization and enhanced thermal stability of paraffin-based phase change materials, RSC Adv. 9 (2019) 9962–9967. https://doi.org/10.1039/C9RA00874H.
[60] Y. Zhang, X. Zhang, R. Bai, X. Hou, J. Li, Interface-Active Metal Organic Frameworks for Knoevenagel Condensations in Water, Catalysts. 8 (2018) 315. https://doi.org/10.3390/catal8080315.
[61] R. Sabouni, H.G. Gomaa, Preparation of Pickering emulsions stabilized by metal organic frameworks using oscillatory woven metal micro-screen, Soft Matter. 11 (2015) 4507–4516. https://doi.org/10.1039/C5SM00922G.
[62] D. Kim, H. Kim, J.Y. Chang, Designing Internal Hierarchical Porous Networks in Polymer Monoliths that Exhibit Rapid Removal and Photocatalytic Degradation of Aromatic Pollutants, Small. 16 (2020) 1907555. https://doi.org/10.1002/smll.201907555.
[63] Y. Zhu, H. Zhang, A. Hui, X. Ye, A. Wang, Fabrication of porous adsorbent via eco-friendly Pickering-MIPEs polymerization for rapid removal of Rb+ and Cs+, Journal of Environmental Chemical Engineering. 6 (2018) 849–857. https://doi.org/10.1016/j.jece.2018.01.010.
[64] M. Kriesten, J.V. Schmitz, J. Siegel, C.E. Smith, M. Kaspereit, M. Hartmann, Shaping of Flexible Metal-Organic Frameworks: Combining Macroscopic Stability and Framework

Flexibility: Shaping of Flexible Metal-Organic Frameworks: Combining Macroscopic Stability and Framework Flexibility, Eur. J. Inorg. Chem. 2019 (2019) 4700–4709. https://doi.org/10.1002/ejic.201901100.

[65] T. Yang, Y. Hu, C. Wang, B.P. Binks, Fabrication of Hierarchical Macroporous Biocompatible Scaffolds by Combining Pickering High Internal Phase Emulsion Templates with Three-Dimensional Printing, ACS Appl. Mater. Interfaces. 9 (2017) 22950–22958. https://doi.org/10.1021/acsami.7b05012.

Figure captions

- **Fig.1.** (a) Pickering emulsions with 2.5 wt.% MIL-96(Al) and different paraffin volume ratios: from left to right, ϕ_v = 0.5, 0.6, 0.7 and 0.8. (b) Pickering emulsions with ϕ_v = 0.8 and different concentrations of MIL-96(Al): from left to right, $w_{\mathrm{MOF}} = 1$, 2, 3.5 and 5 wt.%. Optical micrographs of emulsions with 5 wt.% MIL-96(Al) and paraffin volume ratios of (c) 0.5, (d) 0.6, (e) 0.7, and (f) 0.8.
- **Fig. 2.** Mean droplet sizes (D) in paraffin-in-water emulsions stabilized by MIL-96(Al) as a function of the paraffin volume ratio and the MIL-96(Al) concentration. The error bars represent standard deviations.
- **Fig.3.** Inverse mean droplet diameter (1/D) as a function of mass-to-volume ratio of MIL-96(Al) particles and paraffin in emulsions with paraffin volume ratios of 0.5–0.8 v/v.
- **Fig. 4.** Storage modulus (G'_0) as a function of MIL-96 concentration (wt.%) for emulsions with different paraffin volume ratios.
- **Fig. 5.** Viscosity as a function of the shear rate for (a) emulsions with 2 wt.% MIL-96(Al) and different paraffin volume ratios, and (b, c) emulsions with paraffin volume ratios of 0.6 and 0.8 and different MIL-96(Al) concentrations.
- **Fig.6.** Shear stress as a function of the shear rate for (a) emulsions with 2 wt.% MIL-96(Al) and different paraffin volume ratios, and (b, c) emulsions with paraffin volume ratios of 0.6 and 0.8 and different MIL-96(Al) concentrations.
- **Fig. 7.** Cryo scanning electron micrographs of emulsions with a paraffin volume ratio of 0.8 v/v and MIL-96(Al) concentrations of (a) 1 wt.% and (b) 3.5 wt.%. (1) Continuous aqueous phase concentrated in MIL-96(Al) and (2) oil droplet.

Table

Table 2. Consistency index and power law index obtained by fitting the data in Fig. 5 using Eq. (3)

MIL-96(Al) concentration (wt.%)	Paraffin volume fraction (v/v)	Consistency index K	Power law index n
2	0.5	27.0	0.05
2	0.6	25.5	0.09
2	0.7	56.8	0.09
2	0.8	144.6	0.06
1	0.6	12.4	0.04
3.5	0.6	46.4	0.08
5	0.6	82.1	0.06
1	0.8	90.5	0.08
3.5	0.8	200.9	0.07
5	0.8	245.2	0.06

Graphical abstract